Scattering Functions of Polymeric Core−Shell Structures and Excluded Volume Chains

Stephan Förster* and Christian Burger

Max-Planck-Institut für Kolloid- und Grenzflächenforschung, D-14513 Teltow, Germany

Received May 30, 1997; Revised Manuscript Received November 3, 1997

ABSTRACT: General expressions for the scattering functions of polydisperse particles with an arbitrary number of concentric shells of lamellar, cylindrical, or spherical symmetry are derived. For shells consisting of dense polymer layers or brushes with algebraic density profiles, $\phi(r) \sim r^{\alpha}$, it is possible to obtain closed analytical expressions by taking advantage of the mathematical properties of hypergeometric functions. The same formalism can be employed to derive a closed expression for the form factor of polydisperse excluded volume chains assuming a des Cloizeaux-type segment distribution function.

1. Introduction

By virtue of their way of formation, most colloidal particles are inhomogeneous, often concentric multidomain structures. Prominent examples are micelles, microemulsions, vesicles, dendrimers, or latex particles. The applications of colloidal polymer dispersions are numerous (latex paints, adhesives, flocculants, absorbants, drug carriers) and depend crucially on their size, shape, and surface properties. The analysis of the particle structure is important for the understanding and optimization of industrial processes. From the many methods that are available for the analysis of the internal structure of colloidal particles, scattering techniques (light, X-ray, or neutron) have the longest tradition and have become even more powerful with recent developments of advanced beam sources and detection techniques. The structural analysis of polymeric colloidal particles also helps to understand the basic behavior of polymers confined into microdomains or onto surfaces. To this category belong polymer "brushes", i.e., dense layers of polymer chains tethered to colloidal surfaces. Examples are polymers grafted onto latex particles, the corona of block copolymer micelles, arms of star or comb polymers, or polymers grafted into porous matrices. Such layers play an important role in practical applications such as surface coatings or the steric stabilization of colloids. Their performance as a protective layer strongly depends on their thickness and density profile for which detailed theoretical descriptions have become available in the last decade.[1] Scaling models, originally developed for planar brushes, but later extended to curved interfaces, predict characteristic segment density profiles $\phi(r)$ normal to the interface which are of the general form[2,3]

$$\phi(r) \sim r^{-2(d-1)/3} \tag{1.1}$$

where d is the dimensionality which is $d = 1$ for planar geometry, $d = 2$ for cylinders, and $d = 3$ for spheres. The scaling prediction for the density profile is thus $\phi(r) \sim r^0$ for planar polymer brushes, $\phi(r) \sim r^{-2/3}$ for cylindrical polymer brushes, and $\phi(r) \sim r^{-4/3}$ for spherical polymer brushes. The average brush height $\langle L \rangle$ is directly related to the segment density profile. In the case of planar polymer brushes, self-consistent field theories predict parabolic segment density profiles[4,5]

$$\phi(r) \sim 1 - \left(\frac{r}{\langle L \rangle}\right)^n \tag{1.2}$$

with $n = 2$. Thus algebraic, i.e., r^{α}, density profiles occur quite generally in colloidal polymer systems. The special consideration of such profiles in the analysis of scattering experiments seems quite worthwile. They are expected to be valid for systems with densely grafted polymer chains, i.e., the regime of dense polymer brushes. At small grafting densities ("mushroom" regime), effects of fluctuations, correlation holes close to the (repulsive) grafting surface, and chain-ends altering the density distribution at the outer periphery of the brush become noticable and need to be considered in the calculation of the scattering functions.[1]

Besides algebraic, also exponential density profiles are very common in polymeric systems. The segment distribution function of free polymer chains is of the general form[6]

$$p(r) \sim e^{-r^{\delta}} \tag{1.3}$$

where $\delta = 1/(1 - \nu)$ with ν being the Flory exponent. It is related to the spatial extension R_n of a group of n monomers, which obeys $R_n \sim n^{\nu}$. A flexible chain in an athermal good solvent is characterized by $\nu \approx {}^3/_5$, an ideal coil in a melt is characterized by $\nu = {}^1/_2$, and a collapsed chain in a precipitant is characterized by $\nu = {}^1/_3$. On the other hand, for rigid linear chains we have $\nu = 1$. For the analysis of scattering experiments a wide variety of methods are available ranging from simple linear regressions in Zimm plots[7] to advanced numerical algorithms for inverse Fourier transforms including effects of beam profile and wavelength distribution.[8−11] In many cases, when the particles are expected to exhibit certain types of density profiles such as those discussed above, it is helpful to solve the scattering problem to obtain analytical expressions for the scattering functions to be expected. These functions can be fitted to the measured scattering curves or may serve as a starting point for the evaluation and interpretation of experimental data by solving the inverse scattering problem.

S0024-9297(97)00761-4 CCC: $15.00
Published on Web 01/22/1998

Analytical expressions for the scattering functions of monodisperse homogeneous spheres, cylinders, disks, ellipsoids, and Gaussian chains have been derived many decades ago.[12] While these considered a constant density, Auvray et al. derived expressions for a parabolic density profile[13] to analyze the scattering curves of planar polymer brushes.[14] Expressions for polydisperse spherical[15,16] and monodisperse cylindrical[17] core−shell particles and for polymers grafted onto spherical[18] or ellipsoidal cores[19] are also available.

For the structural analysis of colloidal particles it would be helpful to have a general expression that is valid for different geometries (disks, spheres, cylinders) and density profiles and that takes into account particle polydispersity.

In section 2 we will derive such an expression which is used in section 3 to calculate the form factors of core−shell spheres, cylinders, and disks with algebraic density profiles. The derivation takes advantage of the mathematical properties of hypergeometric functions and is used also in section 4 to calculate the form factor of excluded volume chains.

2. General Formalism

For the following calculations we begin with the relation between form factor $P(q)$, scattered amplitude $F(q)$, and (scattering) density profile $\phi(r)$. The form factor $P(q)$ of a particle is equal to the modulus of the squared amplitude $P(q) = |F^2(q)|$, which for isotropic, finite size particles is given by the Fourier transform of $\phi(r)$ in d dimensions

$$F(q) = F[\phi(r)] = \int \langle \phi(r) \rangle_d \langle e^{iqr} \rangle_d \langle d^d r \rangle_d \qquad (2.1)$$

We will assume an on average centrosymmetric density profile, i.e., $\langle \phi(r) \rangle$ is unchanged by rotations about axes through the center of the particle in d dimensions. For polymeric systems this implies that fluctuations that break centrosymmetry are small, decaying on time scales much shorter than the experimental measuring time. This allows the form factor to be calculated as $P(q) = |F[\langle \phi(r) \rangle]|^2$ using known and simple analytical expressions for $\langle \phi(r) \rangle$. For dense brushes the assumption of centrosymmetry is usually well justified, as the internal relaxation time is of the order of the Rouse relaxation time, which is of the order of microseconds, whereas measuring times are orders of magnitude longer (minutes to hours). Otherwise, if the particles are shape persistent and noncentrosymmetric, as e.g., certain viruses or proteins, the form factor has to be calculated as $P(q) = \langle |F[\phi(r)]|^2 \rangle$ using the corresonding density profiles $\phi(r)$. As a first approximation, the density profile $\phi(r)$ and the phase factor e^{iqr} can then be expanded in spherical harmonics following standard multipole theories.[20] This is, however, beyond the scope of the present paper. During all following calculations, we will assume the density profile to be centrosymmetric and will thus drop the average notation $\langle ... \rangle$.

We will first consider a simple density profile which consists of a number of piecewise analytical functions $\phi(r)$ in each of a number of concentric microdomains of a compartmented particle. Such a profile may be written in the form

$$\phi(r) = \begin{cases} \phi_1(r), & \text{for } R_0 \le r < R_1, \quad \text{domain 1} \\ \phi_2(r), & \text{for } R_1 \le r < R_2, \quad \text{domain 2} \\ ..., & ... \\ \phi_{N+1}(r), & \text{for } R_N \le r < R_{N+1}, \quad \text{domain } N+1 \end{cases} \qquad (2.2)$$

with $R_0 = 0$, $\phi_{N+1} = 0$, and $R_{N+1} = \infty$. The Fourier transform of the density profile can be written as the sum of Fourier transformed density profiles of each domain i

$$F(q) = \frac{\sum_{i=1}^{N+1} F(q,R_i,R_{i-1})}{\sum_{i=1}^{N+1} V(R_i,R_{i-1})} \qquad (2.3)$$

with

$$F(q,R_i,R_{i-1}) = \int_{R_{i-1}}^{R_i} \phi_i(r) \langle e^{iqr} \rangle_d \langle d^d r \rangle_d = F(q,R_i) - F(q,R_{i-1}) \qquad (2.4)$$

$$V(R_i,R_{i-1}) = \int_{R_{i-1}}^{R_i} \phi_i(r) \langle d^d r \rangle_d = V(R_i) - V(R_{i-1}) \qquad (2.5)$$

where $F(q,R) \equiv F(q,R,0)$ and $V(R) \equiv V(R,0)$. For further calculations it is useful to rewrite these functions in terms of hypergeometric functions.

$$F(q,R) = \int_0^R \phi(r)\, {}_0F_1\left(\frac{d}{2}; -\frac{q^2r^2}{4}\right) \frac{2\pi^{d/2}}{\Gamma(d/2)} r^{d-1}\, dr \qquad (2.6)$$

$$V(R) = \int_0^R \phi(r)\, \frac{2\pi^{d/2}}{\Gamma(d/2)} r^{d-1}\, dr \qquad (2.7)$$

which are defined as

$${}_PF_Q(a,b;x) \equiv {}_PF_Q(a_1,a_2,...,a_P,b_1,b_2,...,b_Q;x) \equiv \sum_{n=0}^{\infty} \frac{\prod_{j=1}^{P} (a_j)_n}{\prod_{k=1}^{Q} (b_k)_n} \frac{x^n}{n!} \qquad (2.8)$$

where

$$(a)_n \equiv \frac{\Gamma(a+n)}{\Gamma(a)} = a(a+1)(a+2)\ ...\ (a+n-1) \qquad (2.9)$$

are Pochhammer's factorials. Many special functions (Hermite's, Bessel's, Laguerre's, Legendre's, etc.) can be written in terms of hypergeometric functions and are thus expressible as a series.[21,22] This is often the most practical way to obtain numerical values for these functions.

If $P \le Q$, the sum converges for $x < \infty$ and can be easily calculated via the recurrence relation of the Pochhammer factorial $(a)_{n+1} = (a+n)(a)_n$. This enables an efficient implementation of this function in fitting routines. By using eq 2.8, the integration in eq 2.6 reduces to the problem of integrating a function

$$I(R) = \int_0^R \phi(r) r^{2n+d-1}\, dr \qquad (2.10)$$

which is analytical for many density profiles common

Table 1. Integrals $I(R)$ of the Function r^{2n+d-1} (eq 2.10) over Some Common Distribution Functions $\phi(r)$[a]

$\phi(r)$	$I(R)$	$I(R\to\infty)$
r^{α}	$\frac{1}{d+\alpha+2n}R^{d+\alpha+2n}$	
e^{-ar}	$\frac{1}{a^{d+2n}}\gamma(aR,d+2n)$	$\frac{1}{a^{d+2n}}\Gamma(d+2n)$
$e^{-a^2r^2}$	$\frac{1}{2a^{d+2n}}\gamma\left(a^2R^2,\frac{d}{2}+2n\right)$	$\frac{1}{2a^{d+2n}}\Gamma\left(\frac{d}{2}+n\right)$
$e^{-b(ar)^t}$		$\frac{1}{ta^{d+2n}b^{(d+2n)/t}}\Gamma\left(\frac{d+2n}{t}\right)$

[a] Γ denotes the gamma function, γ the incomplete gamma function.

in polymeric systems such as algebraic $\phi(r) \sim r^{\alpha}$, exponential $\phi(r) \sim e^{-ar}$, Gaussian profiles $\phi(r) \sim e^{-a^2r^2}$, or stretched exponentials $\phi(r) \sim e^{-b(ar)^t}$. Special cases are summarized in Table 1.

Equation 2.10 reveals another useful property of this series expansion. The analysis of scattering curves involves the consideration of particle polydispersity, wavelength distribution, and beam profile. If the corresponding distribution functions $\phi(r)$ are of the types in Table 1, e.g., Schulz−Zimm or Gaussian distributions, then the averaged form factor $\langle P(q)\rangle$ is straightforward to calculate. As an illustration, the particle polydispersity will be explicitely taken into account in the next calculations. In a similar way, Gaussian instrumental resolution functions[23] may be incorporated.

3. Algebraic Density Profiles

In the case of polymer brushes we expect algebraic density profiles as in eq 1.1

$$\phi_i(r) = \rho_i\left(\frac{r}{R_{i-1}}\right)^{\alpha_i} \tag{3.1}$$

where ρ is the interfacial density and R the radius at the interface. For this type of profile, eq 2.3 can be written

$$F(q) = \frac{\sum_{i=1}^{N+1}\rho_i R_{i-1}^{-\alpha_i} F_{\alpha_i}(q,R_i,R_{i-1})}{\sum_{i=1}^{N+1}\rho_i R_{i-1}^{-\alpha_i} V_{\alpha_i}(R_i,R_{i-1})} \tag{3.2}$$

with

$$F_{\alpha_i}(q,R_i,R_{i-1}) = \int_{R_{i-1}}^{R_i} r^{\alpha_i}\langle e^{iqr}\rangle_d\langle d^d r\rangle_d = F_{\alpha_i}(q,R_i) - F_{\alpha_i}(q,R_{i-1}) \tag{3.3}$$

$$V_{\alpha_i}(R_i,R_{i-1}) = \int_{R_{i-1}}^{R_i} r^{\alpha_i}\langle d^d r\rangle_d = V_{\alpha_i}(R_i) - V_{\alpha_i}(R_{i-1}) \tag{3.4}$$

where, similarly as in eqs 2.4 and 2.5, $F_{\alpha}(q,R) \equiv F_{\alpha}(q,R,0)$ and $V_{\alpha}(R) \equiv V_{\alpha}(R,0)$. To prevent a singularity at $r = 0$, α_1 is set equal to zero in the first domain. As the first domain can be made arbitrarily small, this is no serious restriction for further calculations.

Another interesting profile is of the type as in eq 1.2

$$\phi_i(r) = \rho_i\left[1 - \left(\frac{r}{R_i}\right)^{\alpha_i}\right] \tag{3.5}$$

for which a similar expression as eq 3.2 can be derived.

Performing the integration of eqs 3.3 and 3.4 yields the function $F_{\alpha}(q,R)$

$$F_{\alpha}(q,R) = V_{\alpha}(R)\ {}_1F_2\left(\frac{d+\alpha}{2}, \frac{d}{2}, \frac{d+2+\alpha}{2}; -\frac{q^2R^2}{4}\right) \tag{3.6}$$

$$V_{\alpha}(R) = \frac{2\pi^{d/2}}{(d+\alpha)\Gamma(d/2)}R^{d+\alpha} \tag{3.7}$$

Special cases, where $F_{\alpha}(q,R)$ can be expressed in terms of simple trigonometric functions or Bessel functions, are summarized in Table 2.

Since $R_0 = 0$ and $\phi_{N+1} = 0$, the sum over domains in eq 3.2 can be recast in the form

$$F(q,R) = \frac{\sum_{i=1}^{N}\rho_i R_{i-1}^{-\alpha_i} V_{\alpha_i}(R_i)\ {}_1F_2(a_i,b_i;x_i) - \rho_{i+1}R_i^{-\alpha_{i+1}}V_{\alpha_{i+1}}(R_i)\ {}_1F_2(a_{i+1},b_{i+1};x_i)}{\sum_{i=1}^{N}\rho_i R_{i-1}^{-\alpha_i}V_{\alpha_i}(R_i) - \rho_{i+1}R_i^{-\alpha_{i+1}}V_{\alpha_{i+1}}(R_i)} \tag{3.8}$$

which then corresponds to the sum over interfaces i at $r = R_i$. For further calculations it is convenient to introduce the ratio $p_i = R_i/R$, where $R = R_N$ is the outer radius of the particle.

$$F(q,R) = \frac{\sum_{i=1}^{N} p_i^d\left(\left(\frac{p_i}{p_{i-1}}\right)^{\alpha_i}\frac{\rho_i}{d+\alpha_i}\ {}_1F_2(a_i,b_i;x_i) - \frac{\rho_{i+1}}{d+\alpha_{i+1}}\ {}_1F_2(a_{i+1},b_{i+1};x_i)\right)}{\sum_{i=1}^{N} p_i^d\left(\left(\frac{p_i}{p_{i-1}}\right)^{\alpha_i}\frac{\rho_i}{d+\alpha_i} - \frac{\rho_{i+1}}{d+\alpha_{i+1}}\right)} \tag{3.9}$$

with

$${}_1F_2(a_i,b_i;x_j) = {}_1F_2(a_{1,i},b_{1,i},b_{2,i};x_j) = {}_1F_2\left(\frac{d+\alpha_i}{2}, \frac{d}{2}, \frac{d+2+\alpha_i}{2}; -\frac{q^2p_j^2R^2}{4}\right) \tag{3.10}$$

Some special situations are shown schematically in Figure 1. In case (a) the density left of the interface is larger than to the right and the corresponding contribution in the ith term in eq 3.9 is positive. The other case (b) leads to a negative contribution. If, as in case (c), the densities at both sides are equal, i.e., $\rho_{i+1} = (p_i/p_{i-1})^{\alpha_i}$ and $\alpha_i = \alpha_{i+1}$, any discontinuity at the interface vanishes and the corresponding contribution in eq 3.9 becomes equal to zero.

Polydispersity has marked effects on the scattering curve. The measured form factor is then an average $\langle P(q,R)\rangle$ which can be calculated for a given distribution $h(R)$ as

$$\langle P(q,R)\rangle = \langle |F(q)^2|\rangle = \int_0^{\infty} h(R)F^2(q,R)\,\mathrm{d}R \tag{3.11}$$

which, when performed with eq 3.9, leads to a sum of

Table 2. Some Common Cases Where the Hypergeometric Function Reduces to Simple Functions[a]

dim	$\langle e^{iqr}\rangle_d$	$\langle d^d r\rangle_d$	$\phi(r)$	$\frac{F_\alpha(q,R)}{V_\alpha(R)}$
d	${}_0F_1\left(\frac{d}{2};-\frac{q^2R^2}{4}\right)$	$\frac{2\pi^{d/2}r^{d-1}}{\Gamma\left(\frac{d}{2}\right)}$	r^α	${}_1F_2\left(\frac{d+\alpha}{2},\frac{d}{2},\frac{d+2+\alpha}{2};-\frac{q^2R^2}{4}\right)$
1	$\cos(qr)$	2	r^0	${}_0F_1\left(\frac{3}{2};-\frac{q^2R^2}{4}\right)=\Gamma\left(\frac{3}{2}\right)\left(\frac{2}{qR}\right)^{1/2}J_{1/2}(qR)=\frac{\sin(qR)}{qR}$
			r^2	$\frac{3}{(qR)^3}[(qR)^2\sin(qR)-2\sin(qR)+2qR\cos(qR)]$
2	$J_0(qr)$	$2\pi r$	r^0	${}_0F_1\left(2;-\frac{q^2R^2}{4}\right)=\frac{2J_1(qR)}{qR}$
3	$\frac{\sin(qr)}{qr}$	$4\pi r^2$	r^0	${}_0F_1\left(\frac{5}{2};-\frac{q^2R^2}{4}\right)=\Gamma\left(\frac{5}{2}\right)\left(\frac{2}{qR}\right)^{3/2}J_{3/2}(qR)=\frac{3}{(qR)^3}[\sin(qR)-qR\cos(qR)]$
			r^{-1}	$\frac{2}{(qR)^2}[1-\cos(qR)]$

[a] J denotes the Bessel function.

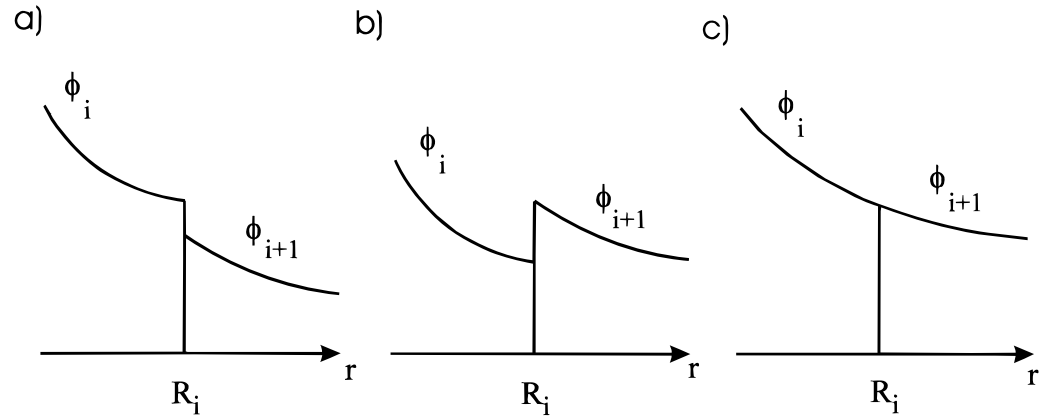

Figure 1. Three examples of density profiles in adjacent domains i and $i+1$. Case (a) leads to a positive term and case (b) to a negative term in the corresponding scattering amplitude in eq 3.9. In case (c) there is no discontinuity at the interface and therefore no contribution to the scattering amplitude; the corresponding term in eq 3.9 is equal to zero.

averages over hypergeometric functions

$$\langle {}_1F_2(a_j,b_j;x_j)\ {}_1F_2(a_{i-j},b_{i-j};x_{i-j})\rangle = \sum_{n=0}^{\infty}\sum_{m=0}^{n}\frac{(a_{1,j})_m(a_{1,i-j})_{n-m}}{(b_{1,j})_m(b_{1,i-j})_{n-m}(b_{2,j})_m(b_{2,i-j})_{n-m}}\times \frac{p_j^{2m}\,p_{i-j}^{2(n-m)}}{m!\,(n-m)!}\left(-\frac{q^2}{4}\right)^n\langle R^{2n}\rangle \quad (3.12)$$

A commonly used distribution function $h(R)$ for polymeric particles is the Schulz–Zimm distribution[24,25] given by

$$h(R)=\frac{(z+1)^{(z+1)}\,R^z}{\langle R\rangle^{z+1}\,\Gamma(z+1)}\exp\left[-(z+1)\frac{R}{\langle R\rangle}\right] \quad (3.13)$$

with the first moment $\langle R\rangle$ and the relative standard deviation $\sigma=(z+1)^{-1/2}$. The distribution is normalized such that $\int_0^\infty h(R)\,dR=1$. The average $\langle R^{2n}\rangle$ for the Schulz–Zimm distribution is

$$\langle R^{2n}\rangle=\frac{\Gamma(z+1+2n)}{\Gamma(z+1)}R_z^{2n}=(z+1)_{2n}\,R_z^{2n} \quad (3.14)$$

with $R_z=\langle R\rangle/(z+1)$. Inserting eq 3.14 in eq 3.12 leads to the final expression

$$\langle {}_1F_2(a_j,b_j;x_j)\ {}_1F_2(a_{i-j},b_{i-j};x_{i-j})\rangle = \sum_{n=0}^{\infty}\sum_{m=0}^{n}\frac{(a_{1,j})_m(a_{1,i-j})_{n-m}(z+1)_{2n}}{(b_{1,j})_m(b_{1,i-j})_{n-m}(b_{2,j})_m(b_{2,i-j})_{n-m}}\times \frac{p_j^{2m}\,p_{(i-j)}^{2(n-m)}}{m!(n-m)!}\left(-\frac{q^2\,R_z^2}{4}\right)^n \quad (3.15)$$

which inserted in eqs 3.9 and 3.11 gives a general expression for the form factor of a d-dimensional polydisperse particle with N concentric domains, each with an algebraic density profile of the form r^{α_i}.

An important parameter that characterizes the size of a particle is its radius of gyration, R_g. For a particle with finite outer radius R it can be calculated as

$$R_g^2=\frac{1}{V(R)}\int_0^R r^2\phi(r)\,\langle d^d r\rangle_d \quad (3.16)$$

Using the general expression for the volume element $\langle d^d r\rangle_d$ in Table 2 together with algebraic density profile $\phi(r)$ in eq 3.1, one obtains for a particle of N concentric

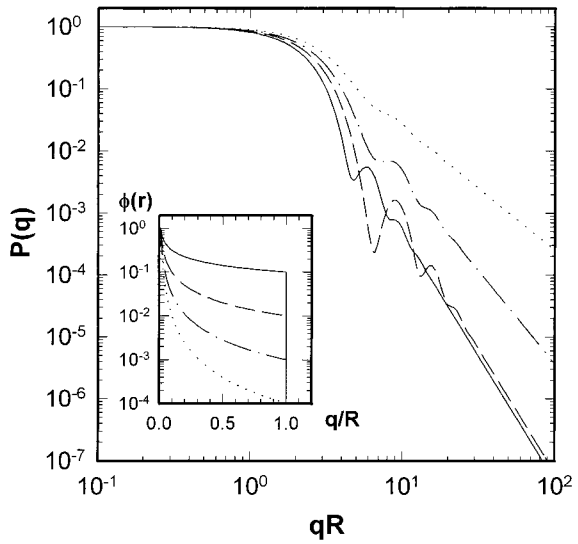

Figure 2. Calculated form factor $P(q)$ (eq 3.18) for hyperbolic density profiles r^{α} with $\alpha = -0.5$ (solid line), $\alpha = -1.0$ (dashed line), $\alpha = -1.5$ (dash-dotted line), and $\alpha = -2.0$ (dotted line). Note the characteristic steep first minimum of the $\alpha = -1.0$ profile. The insert shows the density profiles.

shells with outer radius R

$$R_g^2 = \frac{\sum_{i=1}^{N} p_i^{d+2}\left(\left(\frac{p_i}{p_{i-1}}\right)^{\alpha_i}\frac{\rho_i}{d+2+\alpha_i} - \frac{\rho_{i+1}}{d+2+\alpha_{i+1}}\right)}{\sum_{i=1}^{N} p_i^{d}\left(\left(\frac{p_i}{p_{i-1}}\right)^{\alpha_i}\frac{\rho_i}{d+\alpha_i} - \frac{\rho_{i+1}}{d+\alpha_{i+1}}\right)} R^2 \quad (3.17)$$

With the Schulz−Zimm distribution one can calculate R_g of a polydisperse particle using eq 3.14 as $\langle R_g^2\rangle = ((z + 2)/(z + 1))R_g^2$. To illustrate typical features of scattering curves of spherical polymer brushes with r^{α} profiles, we calculated the form factor of a simple spherical polymer brush

$$P(q) = \left\langle {}_1F_2^2\left(\frac{3+\alpha}{2}, \frac{3}{2}, \frac{5+\alpha}{2}; -\frac{q^2 R^2}{4}\right)\right\rangle \quad (3.18)$$

for various values of α in Figure 2. We note the characteristic steep first minimum of the r^{-1} profile and the increase of the oscillation period with increasing α. Both features have been experimentally observed for block copolymer micelles that represent model systems for dense spherical polymer brushes.[31]

Even for dense brushes, effects of fluctuations around the average density profile will become noticable at large q-values or short distances. In the following we will briefly outline approximate treatments.

Similar to semidilute solutions, the brush domains can be viewed as a melt of blobs of diameter ξ. In order to estimate the contribution of fluctuation effects, the particle structure is assumed to be governed by two different length scales, i.e., the particle radius R and the blob size ξ.[32] If the length scales are sufficiently different, the form factor $P(q)$ can be expressed as the sum of the form factor due to particle shape scattering, $P_p(q)$, and the form factor due to fluctuations, $P_f(q)$

$$P(q) = P_p(q) + P_f(q) \quad (3.19)$$

If length scales are similar, cross-terms between both contributions have to be considered as well.[18] $P_p(q)$ corresponds to the dense brush form factors derived above (eq 3.11), but also the Guinier expression[33] or the solid sphere form factor[18] have been used. As in semidilute solutions where excluded volume interactions are fully screened, $P_f(q)$ is of the Ornstein−Zernike form,[6] i.e., $P_f(q) \sim (q^2 + \xi^{-2})^{-1}$ exhibiting a characteristic q^{-2}-asymptote. If excluded volume interactions are not fully screened, $P_f(q)$ has a $q^{-1/\nu}$ -asymptote where ν is the Flory exponent. An expression for the corresponding scattering function has been given by Dozier et al.[33] The form factor of an excluded volume chain is considered in more detail in section 4.

$P_f(q)$ will dominate the scattered intensity for $q\xi_m \gg 1$ where ξ_m is the blob size at the periphery of the particle. ξ_m is of the order of $R_f^{-1/2}$ for spherical, $R\xi_g$ for cylindrical, and ξ_g^2 for planar polymer brushes, where R is the particle radius, ξ_g the grafting density of the cylinder or plane, and f the aggregation number of block copolymer micelles or the number of arms of star polymers. Throughout the next sections, we will only consider the scattering in the regime $q\xi_m \ll 1$, which reflects the typical features of core−shell particles and dense polymer brushes. Fluctuations will contribute a $q^{-1/\nu}$-asymptote at larger q until the scattering contribution due to the cross section of the polymer backbone becomes dominant.

We will consider simple core−shell particles ($N = 2$) with a core of constant density, i.e., $\alpha_1 = 0$. In this case eq 3.11 with eqs 3.9 and 3.15 reduces to

$$\begin{aligned}\langle P(q)\rangle = \frac{1}{\sum_{i=1}^{6} c_i}(&c_1\langle {}_1F_2(a_0,b_0;x_1)\ {}_1F_2(a_0,b_0;x_1)\rangle + \\ &c_2\langle {}_1F_2(a_0,b_0;x_1)\ {}_1F_2(a_2,b_2;x_2)\rangle + \\ &c_3\langle {}_1F_2(a_0,b_0;x_1)\ {}_1F_2(a_2,b_2;x_1)\rangle + \\ &c_4\langle {}_1F_2(a_2,b_2;x_2)\ {}_1F_2(a_2,b_2;x_2)\rangle + \\ &c_5\langle {}_1F_2(a_2,b_2;x_2)\ {}_1F_2(a_2,b_2;x_1)\rangle + \\ &c_6\langle {}_1F_2(a_2,b_2;x_1)\ {}_1F_2(a_2,b_2;x_1)\rangle)\end{aligned} \quad (3.20)$$

with $a_0 = a(\alpha{=}0)$ and $b_0 = b(\alpha{=}0)$ and

$$c_1 = \frac{\rho_1^2}{d^2}$$

$$c_2 = 2\,\frac{p_1^{-(d+\alpha_2)}\rho_1\rho_2}{d(d+\alpha_2)}$$

$$c_3 = -2\,\frac{\rho_1\rho_2}{d(d+\alpha_2)}$$

$$c_4 = \frac{p_1^{-2(d+\alpha_2)}\rho_2^2}{(d+\alpha_2)^2}$$

$$c_5 = -2\,\frac{p_1^{-(d+\alpha_2)}\rho_2^2}{(d+\alpha_2)^2}$$

$$c_6 = \frac{\rho_2^2}{(d+\alpha_2)^2}$$

According to eq 3.17 the radius of gyration is

$$R_g^2 = \frac{\left(\frac{\rho_1}{d+2} + \frac{\rho_2}{d+2+\alpha_2}(p_1^{-(d+2+\alpha_2)} - 1)\right)}{\left(\frac{\rho_1}{d} + \frac{\rho_2}{d+\alpha_2}(p_1^{-(d+\alpha_2)} - 1)\right)} p_1^2 R^2 \tag{3.21}$$

Many experiments can be performed under index-matching conditions, meaning that either ρ_1 or ρ_2 can be made arbitrarily small. In the following we will consider three interesting cases:

Case 1. $\rho_2 = 0$ corresponds to index matching of the shell. In this case we have the scattering of the core

$$\langle P(q)\rangle = \langle {}_1F_2(a_0,b_0;x_1)\ {}_1F_2(a_0,b_0;x_1)\rangle \tag{3.22}$$

with the radius of gyration

$$R_g^2 = \frac{d}{d+2}(p_1 R)^2 \tag{3.23}$$

which yields the well-known result $R_g = (^3/_5)^{1/2} p_1 R \approx 0.775 p_1 R$.

Case 2. In the case $\rho_1 = 0$ the core is index matched and we observe the scattering of the shell

$$\langle P(q)\rangle = \frac{1}{c}(p_1^{-2(d+\alpha_2)}\langle {}_1F_2(a_2,b_2;x_1)\ {}_1F_2(a_2,b_2;x_1)\rangle - 2p_1^{-(d+\alpha_2)}\langle {}_1F_2(a_2,b_2;x_1)\ {}_1F_2(a_2,b_2;x_2)\rangle + \langle {}_1F_2(a_2,b_2;x_2)\ {}_1F_2(a_2,b_2;x_2)\rangle) \tag{3.24}$$

with $c = p_1{}^{-2(d+\alpha_2)} - 2p_1{}^{-(d+\alpha_2)} + 1$and the radius of gyration

$$R_g^2 = \frac{d+\alpha_2}{d+2+\alpha_2}\frac{(p_1^{-(d+2+\alpha_2)} - 1)}{(p_1^{-(d+\alpha_2)} - 1)}(p_1 R)^2 \tag{3.25}$$

Case 3. Another interesting case is that of a vanishing discontinuity at the interface, i.e., $\rho_2 = \rho_1{}^{-\alpha_i}$ with $\alpha_1 = \alpha_2$

$$\langle P(q)\rangle = \langle {}_1F_2(a_0,b_0;x_2)\ {}_1F_2(a_0,b_0;x_2)\rangle \tag{3.26}$$

with the radius of gyration

$$R_g^2 = \frac{d}{d+2} R^2 \tag{3.27}$$

The simplest example for a parabolic brush profile as in eq 3.5 is a single domain particle with radius R. Then the form factor becomes

$$\langle P(q)\rangle = \frac{1}{c}\left(\frac{1}{d^2}\langle {}_1F_2(a_0,b_0;x_1)\ {}_1F_2(a_0,b_0;x_1)\rangle - \frac{2}{d(d+\alpha_2)}\langle {}_1F_2(a_0,b_0;x_1)\ {}_1F_2(a_2,b_2;x_1)\rangle + \frac{1}{(d+\alpha_2)^2}\langle {}_1F_2(a_2,b_2;x_1)\ {}_1F_2(a_2,b_2;x_1)\rangle\right) \tag{3.28}$$

with $c = (1/d^2) - (2/d(d+\alpha_2)) + (1/(d+\alpha_2)^2)$ and the radius of gyration

$$R_g^2 = \frac{\left(\frac{1}{d+2} - \frac{1}{d+2+\alpha}\right)}{\left(\frac{1}{d} - \frac{1}{d+\alpha}\right)}(p_1 R)^2 \tag{3.29}$$

Some special cases of eq 3.20 have been considered previously. The case of a polydisperse spherical ($d = 3$) core−shell particle with constant densities in each domain ($\alpha_1 = \alpha_2 = 0$) has been derived by Hayter[15] and was used to analyze scattering curves of surfactant micelles by Huang et al.[16] The case of a monodisperse cylindrical ($d = 2$) core−shell particle with constant densities ($\alpha_1 = \alpha_2 = 0$) has been calculated by Mittelbach and Porod.[17]

It is straighforward to write down form factors also for three or more domain particles. Examples could be particles with an extended interfacial region with some characteristic density profile or particles with a two-domain shell structure as expected for starlike[26] or micellar[27] polymer structures.

In the following sections we will consider the special cases of core−shell particles ($N = 2$) of spherical ($d = 3$), cylindrical ($d = 2$), or lamellar ($d = 1$) shape and arbitrary ρ, p, and α. All calculations are performed with eq 3.20 or eq 3.28 depending on the type of density profile, i.e., eq 3.1 or eq 3.5.

3.1. Spherical Particles. We will consider a simple density profile $\phi(r)$ expected for a spherical particle with a solid core and a polymeric shell. Examples for such particles would be sterically stabilized latex particles, block copolymer micelles or star polymers. Such a density profile can be written according to eq 2.2 with $\rho_1 = \rho_c$, $\rho_2 = \rho_s$, $\alpha_1 = 0$, $\alpha_2 = \alpha$, $R_1 = R_c$, and $R_2 = R$

$$\phi(r) = \begin{cases} \rho_c, & \text{for } 0 \le r < R_c \quad \text{(core)} \\ \rho_s\left(\frac{r}{R_c}\right)^{-\alpha}, & \text{for } R_c \le r < R \quad \text{(shell)} \\ 0, & \text{for } R \le r \end{cases} \tag{3.30}$$

where ρ_c is the core density, ρ_s the density at the core−shell interface, R_c the core radius, and R the outer radius of the particle. The shell has the typical algebraic density profile of a polymeric brush. Given these structural parameters together with the polydispersity σ, one calculates the constants a_i, b_i, and c_i in eq 3.20 for the case of spherical particles ($d = 3$) to obtain the form factor $P(q)$. Each of the six averages $\langle {}_1F_2(a_i,b_i;x_j)\ {}_1F_2(a_k,b_k;x_l)\rangle$ is given by the double sum in eq 3.15 where 10−20 terms are sufficient for an accuracy of 10^{-6}. For $x_i > 10$ the asymptotic expansion given in the Appendix is used. As an illustration we show in Figure 3 the calculated form factors for particles with a $r^{-4/3}$ shell profile as expected for spherical polymer brushes.

The core radius is $R_c/R = 0.3$ and polydispersity $\sigma = 0.1$, which are typical values for colloidal particles. The case $\rho_s = 0$ corresponds to a solid sphere of radius R_c which, as seen in Figure 3, shows the expected oscillations with a Porod q^{-4} envelope. With increasing interfacial density ρ_s, one notes the appearance of a minimum at $qR \approx 7$ and change of the slope at large q typical for hyperbolic polymer brushes. For the simple case of a solid sphere with radius R_c the expression in

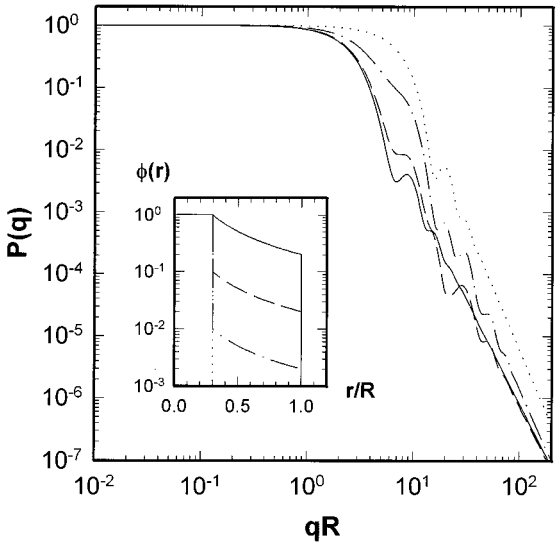

Figure 3. Calculated form factor $P(q)$ (eq 3.20) for spheres ($d = 3$) with a solid core and a shell with a $r^{-4/3}$ profile characteristic for spherical polymer brushes (eq 3.30). The core radius is $R_c/R = 0.3$, the relative standard deviation $\sigma = 0.1$. Interfacial densities are $\rho_2 = 1.0$ (solid line), $\rho_2 = 0.1$ (dashed line), $\rho_2 = 0.01$ (dash-dotted line), and $\rho_2 = 0$ (dotted line). The last case represents the scattering of just the solid core. The insert shows the density profiles.

eq 3.9 reduces in the case of monodisperse particles

$$\frac{F(q,R_c)}{V(R_c)} = \frac{1}{(4\pi/3)\,R_c^3}\int_0^{R_c}\frac{\sin(qr)}{qr}\,4\pi r^2\,\mathrm{d}r = \frac{3}{(qR_c)^3}[\sin(qR_c) - qR_c\cos(qR_c)] \quad (3.31)$$

the classical expression derived by Rayleigh.[28] Other cases where $F(q)$ reduces to simple trigonometric functions are also tabulated in Table 2 as, e.g., in the case r^{-1} expected for dense spherical polymer brushes.

3.2. Cylindrical Particles. Equation 3.20 can also be used to calculate the form factors of cylindrical core−shell particles ($d = 2$). For cylinders with length L and radius R the form factor can be factorized into

$$P(q) = P_L(q)P_x(q) = P_L(q)|F_x^2(q)| \quad (3.32)$$

if the axial ratio $L/R > 10$.[10] $P_L(q)$ is the orientationally averaged form factor of an infinitely thin rod[29]

$$P_L(q) = \frac{2}{qL}\,\mathrm{Si}(qL) - \left(\frac{\sin(qL/2)}{qL/2}\right)^2 \quad (3.33)$$

with $\mathrm{Si}(qL)$ the sine integral. This function has an asymptote

$$\lim_{qL\to\infty} P_L(q) = \frac{\pi}{qL}$$

$P_x(q)$ is the cross-sectional form factor. The corresponding amplitude $F_x(q)$ is equal to the case $d = 2$ in eq 3.20. As an illustration we calculate the form factor of cylindrical core-shell particles with the same density profile as in the case of spherical particles (eq 3.30), but with a value $\alpha = -2/3$ characteristic for cylindrical polymer brushes. Examples for different interfacial densities ρ_s are shown in Figure 4.

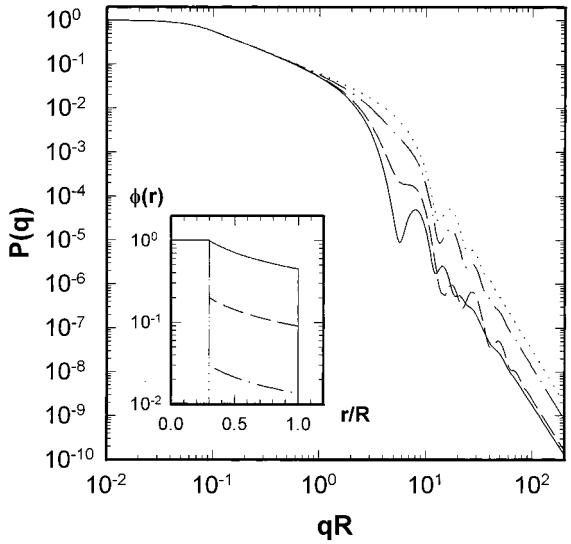

Figure 4. Calculated form factor $P(q)$ (eq 3.20) for cylinders ($d = 2$) with a solid core and a shell with a $r^{-2/3}$ profile characteristic for cylindrical polymer brushes (eq 3.30). The length of the cylinder is $L/R = 50$. The core radius is $R_c/R = 0.3$, the relative standard deviation $\sigma = 0.1$. Interfacial densities are $\rho_2 = 1.0$ (solid line), $\rho_2 = 0.2$ (dashed line), $\rho_2 = 0.03$ (dash-dotted line), and $\rho_2 = 0$ (dotted line). The last case represents the scattering of just the solid cylindrical core. The insert shows the density profiles.

The case $\rho_s = 0$ corresponds to a solid cylinder of radius R_c whose scattering curve shows the typical oscillations with a Porod q^{-4}-envelope. With increasing interfacial density we observe the appearance of a minimum at $qR \approx 6$. In the case $\rho_2 = 0$ the expression in eq 3.9 reduces to

$$\frac{F_x(q,R_c)}{V_x(R_c)} = \frac{1}{\pi R_c^2}\int_0^{R_c} J_0(qr)2\pi r\,\mathrm{d}r = \frac{2J_1(qR_c)}{qR_c} \quad (3.34)$$

for monodisperse particles which is the well-known expression derived by Neugebauer.[29]

3.3. Lamellar Particles. Equation 3.20 is also applicable to disk or sheetlike particles corresponding to the case $d = 1$. For disks of radius D and thickness $2R$, the form factor can be factorized into

$$P(q) = P_D(q)P_x(q) = P_D(q)|F_x^2(q)| \quad (3.35)$$

if the axial ratio $D/R > 10$. $P_D(q)$ is the orientationally averaged form factor of an infinitely thin disk of radius D[30]

$$P_D(q) = \frac{2}{(qD)^2}\left(1 - \frac{J_1(2qD)}{qD}\right) \quad (3.36)$$

which has an asymptote

$$\lim_{qD\to\infty} P_D(q) = \frac{2}{(qD)^2}$$

$P_x(q)$ is the thickness form factor normal to the disk. Its corresponding amplitude $F_x(q)$ is equal to the case $d = 1$ in eq 3.20. One can use again the density profile in eq 3.30 to calculate the form factors of core−shell planar particles with, e.g., a characteristic profile r^0 as expected for planar polymer brushes. The case $\rho_2 = 0$ would then correspond to a solid disk of thickness $2R_c$

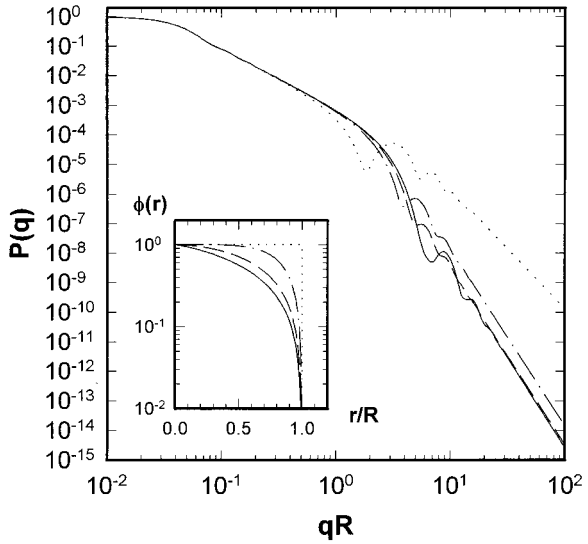

Figure 5. Calculated form factor $P(q)$ (eq 3.28) for disks ($d = 1$) with a $1 - (r/R)^{\alpha}$ profile characteristic for planar polymer brushes. The radius of the disk is $R_D/R = 50$, the relative standard deviation is $\sigma = 0.1$. The form factors are calculated for $\alpha = 1.2$ (solid line), $\alpha = 1.8$ (dashed line), $\alpha = 4.8$ (dash-dotted line), and $\alpha \rightarrow \infty$ (dotted line). The last case corresponds to the scattering of a solid disk. The insert shows the density profiles.

for which eq 3.9 reduces to

$$\frac{F_x(q,R_c)}{V_x(R_c)} = \frac{1}{2R_c}\int_0^{R_c} 2\cos(qr)\,\mathrm{d}r = \frac{\sin(qR_c)}{qR_c} \qquad (3.37)$$

in the case of monodisperse particles as derived by Kratky and Porod.[30]

We now consider disklike particles consisting of a core with a parabolic density profile expected for planar polymer brushes as in eq 3.5. For large brush densities such profiles approach a simple step profile. The corresponding scattering curve is given by eq 3.28. As an illustration we calculate the form factors for various values of α in Figure 5.

We note the typical q^{-6}-asymptotes of such profiles, due to the cancellation of the q^{-4}-terms in eq 3.28. If $\alpha \rightarrow \infty$, $\phi(r)$ approaches a step profile with the corresponding scattering curve of a solid disk with a Porod q^{-4}-envelope. The case $\alpha = 2$ has a solution in terms of trigonometric functions given in Table 2, which has been derived previously by Auvray et al.[13]

4. Excluded Volume Chain

The excluded volume or self-avoiding effect of polymer chains is one of the classical problems in polymer physics. In the presence of excluded volume, the probability distribution function $P(r)$ of the distance r between two monomers differs from the Gaussian distribution. Approximate expressions for the probability distribution function have been derived either from renormalization group (RNG) calculations or from Monte Carlo (MC) simulations. It is now commonly accepted that the distribution function suggested by des Cloizeaux,[34,35]

$$p(r) \sim r^{2+\theta_s} \exp[-r^{\delta_s}] \qquad (4.1)$$

with the exponents $\delta_s = 1/(1 - \nu_s)$ and $\theta_s = (\gamma_s - 1)/\nu_s$ gives the best description of an excluded volume chain.[36,37] The two critical exponents γ and ν are related to the chain entropy and the chain size, respectively.[6] In the long chain limit, their value only depends on the dimensionality d: $\gamma = {}^7/_6$ for $d = 3$, $\gamma = {}^4/_3$ for $d = 2$, and $\gamma = 1$ for $d = 1$. For ν there is a simple relation $\nu = 3/(d + 2)$ to the dimensionality d.[38] From RNG theory the best estimates for $d = 3$ are currently $\nu = 0.588$ and $\gamma = 1.1619$.[39]

For chains of finite length, des Cloizeaux has shown that the values of the critical exponents depend on the actual position of the chain segments on the chain contour. Three principal cases where a subchain contains no chain ends ($s = 0$), one chain end ($s = 1$), or both chain ends ($s = 2$) can be distinguished. Wittkop et al.[46] obtained from MC simulations different values of ν_s ($\nu_0 = 0.592$, $\nu_1 = 0.615$, $\nu_2 = 0.623$) for each case.

Some approximate expressions for the form factor of excluded volume chains have been derived[40−43] and are discussed in ref 44. The most general expression was given in the form of a series expansion by Utiyama et al.,[43] derived from a distribution function of the type (4.1). Such distribution functions neglect the local stiffness of polymer chains. The corresponding form factors are therefore valid only for $qb < 1$, where b is the segment length. Effects of chain stiffness on the form factor of excluded volume chains have recently been considered in detail by Pedersen and Schurtenberger.[45]

In the following we will derive the form factor of an excluded volume chain in the long chain limit by using eq 2.6 together with the distribution function $p(r)$ of eq 4.1, which is normalized as[46]

$$P(r) = \frac{1}{X_s^d} B_s \left(\frac{r}{X_s}\right)^{2+\theta_s} \exp\left[-D_s\left(\frac{r}{X_s}\right)^{\delta_s}\right] \qquad (4.2)$$

with $X_s = (\langle R_s^2\rangle/d)^{1/2}$. The normalization constants are obtained from the conditions $\int_0^\infty P(r)\langle d^d r\rangle_d = 1$ and $\int_0^\infty r^2 P(r)\langle d^d r\rangle_d = \langle R_s^2\rangle$ yielding

$$D_s = \left[\frac{1}{d}\frac{\Gamma\left(\dfrac{4 + d + \theta_s}{\delta_s}\right)}{\Gamma\left(\dfrac{2 + d + \theta_s}{\delta_s}\right)}\right]^{\delta_s/2} \qquad (4.3)$$

$$B_s = \frac{\delta_s \Gamma\left(\dfrac{d}{2}\right)}{2\pi^{d/2}} \frac{D_s^{(2+d+\theta_s)/\delta_s}}{\Gamma\left(\dfrac{2 + d + \theta_s}{\delta_s}\right)} \qquad (4.4)$$

with $\langle R_s^2\rangle$ where ν is Flory's exponent and b the statistical segment length. Note that the distribution function $P(r)$ differs by a factor X_s^{-d} from the distribution function used by Utiyama et al.[43]

In the case $\delta_s = 2$, $\theta_s = -2$, and $d = 3$, eq 4.2 reduces to the Gaussian distribution function

$$P(r) = \left(\frac{3}{2\pi\langle R_s^2\rangle}\right)^{3/2} \exp\left[-\frac{3r^2}{2\langle R_s^2\rangle}\right] \qquad (4.5)$$

The Fourier transform is calculated by employing eq 2.6, i.e.

$$F(q,R) = \int_0^\infty P(r)\ {}_0F_1\left(\frac{d}{2}; -\frac{q^2r^2}{4}\right)\frac{2\pi^{d/2}}{\Gamma(d/2)}\, r^{d-1}\, \mathrm{d}r \qquad (4.6)$$

to obtain

$$F(q) = A_s \sum_{n=0}^{\infty} \frac{\Gamma\left(\dfrac{2+d+\theta_s+2n}{\delta_s}\right)}{\Gamma\left(\dfrac{d}{2}+n\right)} \frac{\left(-\dfrac{q^2X_s^2}{4D_s^{2/\delta_s}}\right)^n}{n!} \qquad (4.7)$$

with

$$A_s = \frac{2\pi^{d/2}B_s}{\delta_s D_s^{(2+d+\theta_s)/\delta_s}} \qquad (4.8)$$

In the case $\delta_s = 2$, $\theta_s = -2$, and $d = 3$, eq 4.7 reduces to the Gaussian

$$F(q) = \exp\left[-\frac{q^2X_s^2}{2}\right] \qquad (4.9)$$

To obtain the form factor, $F(q)$ is integrated over the contour of the excluded volume chain

$$P(q) = \frac{2}{N^2}\int_0^N (N-n)F(q)\, \mathrm{d}n \qquad (4.10)$$

where N is the total number of segments of the excluded volume chain. This neglects chain end effects that lead to different values of the critical exponents as discussed above. Equation 4.10 is therefore expected to be valid in the long chain limit. In a similar way the radius of gyration, R_g, is calculated

$$R_g^2 = \frac{1}{N^2}\int_0^N (N-n)\langle R_s^2\rangle\, \mathrm{d}n = \frac{b^2N^{2\nu}}{(1+2\nu)(2+2\nu)} \qquad (4.11)$$

which in the cases $\nu = {}^1/_2$ and $\nu = 1$ reduce to the expressions for a Gaussian chain, $R_g^2 = Nb^2/6$, and a rodlike particle, $R_g^2 = N^2b^2/12$, respectively. Evaluation of the integral in eq 4.10 leads to the form factor of the excluded volume chain

$$P(q) = 2A_s \sum_{n=0}^{\infty} \times \frac{\Gamma\left(\dfrac{2+d+\theta_s+2n}{\delta_s}\right)}{\Gamma\left(\dfrac{d}{2}+n\right)} \frac{(1+2\nu)^n(2+2\nu)^n}{(1+2\nu n)(2+2\nu n)} \frac{\left(-\dfrac{q^2R_g^2}{4dD_s^{2/\delta_s}}\right)^n}{n!} \qquad (4.12)$$

In the Gaussian limit ($\delta_s = 2$, $\theta = -2$, $d = 3$) it yields the Debye form factor[47]

$$P(q) = 2\sum_{n=0}^{\infty}\frac{(-x)^n}{(n+2)!} = 2\left(\frac{e^{-x}}{x^2} + \frac{1}{x} - \frac{1}{x^2}\right) \qquad (4.13)$$

where $x = q^2R_g^2$. The asymptotic expansion has a leading term

$$\lim_{x\to\infty} P(q) = A_s \frac{\Gamma\left(\dfrac{1}{2\nu}\right)\Gamma\left(\dfrac{2+d+\theta_s}{\delta_s} - \dfrac{1}{\nu\delta_s}\right)}{\nu\Gamma\left(\dfrac{d}{2} - \dfrac{1}{2\nu}\right)} \times \left(\frac{(1+2\nu)(2+2\nu)x}{4dD_s^{\delta_s/2}}\right)^{-1/(2\nu)} \qquad (4.14)$$

which exhibits the expected $(qR_g)^{-1/\nu}$ behavior. In the Gaussian limit it reduces to the well-known asymptotic

$$\lim_{x\to\infty} P(q) = \frac{2}{x} \qquad (4.15)$$

behavior. For polydisperse chains where the degree of polymerization N exhibits a Schulz−Zimm distribution, it is possible to derive analytic expressions for the scattering function. The polydispersity index z of the Schulz−Zimm distribution is closely related to the parameter $M_w/M_n = (z+2)/(z+1)$, which is often used to characterize the polydispersity of polymers.

Using the Schulz−Zimmm distribution together with the relation between R_g and N from eq 4.11 the R_g^{2n} term in eq 4.12 becomes

$$\langle R_g^{2n}\rangle = \frac{\Gamma(z+1+2\nu n)}{\Gamma(z+1)\,(z+1)^{2\nu n}}\, R_g^{2n} = \frac{(z+1)_{2\nu n}}{(z+1)^{2\nu n}}\, R_g^{2n} \qquad (4.16)$$

This can be inserted into eq 4.12 to obtain the form factor of a polydisperse excluded volume chain

$$P(q) = 2A_s \sum_{n=0}^{\infty} \frac{\Gamma\left(\dfrac{2+d+\theta_s+2n}{\delta_s}\right)}{\Gamma\left(\dfrac{d}{2}+n\right)} \times \frac{(1+2\nu)^n(2+2\nu)^n(z+1)_{2\nu n}}{(1+2\nu n)(2+2\nu n)} \frac{\left(-\dfrac{q^2R_g^2}{4d(z+1)^{2\nu}D_s^{2/\delta_s}}\right)^n}{n!} \qquad (4.17)$$

with the radius of gyration

$$\langle R_g^2\rangle = \frac{\Gamma(z+1+2\nu)}{\Gamma(z+1)(z+1)^{2\nu}}\, R_g^2 \qquad (4.18)$$

Note that in the case of Gaussian chains ($\nu = {}^1/_2$) $\langle R_g^2\rangle$ and R_g^2 are identical. The form factor of the

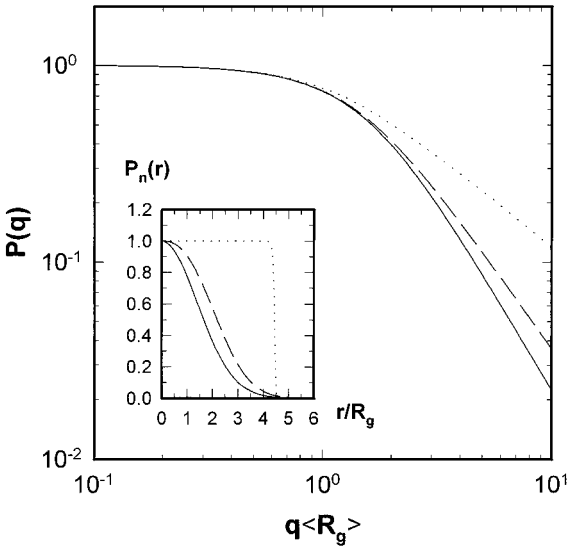

Figure 6. Calculated form factor $P(q)$ of polydisperse excluded volume chains with $\nu = {}^1/_2$ (solid line), $\nu = {}^3/_5$ (dashed line), and $\nu = 0.99$ (dotted line). The relative standard deviation in the degree of polymerization or contour length is $\sigma = 0.35$ corresponding to a polydispersity of $M_w/M_n = 1.12$. The insert shows the density profiles, normalized to $P_n(0) = 1$.

polydisperse excluded volume chain has an asymptote (see Appendix)

$$\lim_{x\to\infty} P(q) = A_s \frac{\Gamma\left(\frac{1}{2\nu}\right)\Gamma\left(\frac{2+d+\theta_s}{\delta_s} - \frac{1}{\nu\delta_s}\right)}{\nu z \Gamma\left(\frac{d}{2}\frac{1}{2\nu}\right)} \times \left(\frac{(1+2\nu)(2+2\nu)x}{4d(z+1)^{2\nu}D_s^{2/\delta_s}}\right)^{-1/(2\nu)} \quad (4.19)$$

Thus for large values of qR_g one still has a $(qR_g)^{-1/\nu}$ behavior. In the Gaussian limit the asymptote reduces to

$$\lim_{x\to\infty} P(q) = \frac{2(z+1)}{z}\frac{1}{x} \quad (4.20)$$

For monodisperse chains $z \to \infty$, and one obtains eq 4.15.

As an example we calculated the form factors of polydisperese excluded volume chains for different values of ν in Figure 6.

We note the characteristic $q^{-1/\nu}$ profiles of these scattering curves. The series expansion together with the asymptotic expansion allows the calculation of the form factor over the entire q-range. The insert shows the probability distribution function $P(r)$ normalized to $P(0) = 1$ to illustrate the evolution into a step function as ν approaches unity. One does not obtain the form factor of a rigid rod (eq 3.33) for $\nu = 1$, since $P(r)$ was assumed to be isotropic.

5. Conclusions

By using hypergeometric functions we have derived general expressions for the form factor $P(q)$ of core−shell particles of various shapes and density profiles. Expressions such as eqs 3.20 and 3.28 are given as series expansions which are valid for polydisperse core−shell particles of various geometries (spheres, cylinders, disks) with algebraic density profiles. We have also calculated the asymptotic expansions which allow calculation of the form factors over the entire q-range. These expressions are straightforward to implement in routines for the analysis of scattering curves. The same formalism has been used to calculate the form factor (eq 4.17) of polydisperse excluded volume chains starting from the des Cloizeaux segment distribution function. The derived scattering functions should quite generally be applicable for densely grafted spheres, cylinders, and disks. The form factors are completely defined in terms of parameters related to particle structure such as size, density, and polydispersity. Similarly, the form factor for the excluded volume chain is given in terms of the degree of polymerization, polydispersity, and the two critical exponents γ and ν. These scattering functions have already been successfully used to analyze the structure of spherical[31] and wormlike block copolymer micelles.[48] It is the hope of the authors that this approach can also be used for the analysis of other colloidal or polymeric structures and that potential users are not distracted from the use of less common transcendental functions.

Acknowledgment. We thank M. Antonietti and H. Schnablegger for many helpful suggestions.

Appendix

The procedure to calculate form factors via hypergeometric functions seems involved but is in fact quite straightfoward. As an example one may take eq 3.20, which yields the form factor of a core-shell particle with a solid core. The specification of the set of structural parameters ρ_1, ρ_2, p_1, α_2, R, and d enables the calculation of the coefficients c_1−c_6 and the arguments a_1, b_1, b_2, and x (see eq 3.10) of the hypergeometric functions. The averages $\langle ... \rangle$ are given by the double sum in eq 3.15 where the polydispersity index z needs to be specified. The double summation converges quickly; 10−20 terms are sufficient for an accuracy of 10^{-6}. At large q the summation breaks down due to rounding errors. This is not a problem since the hypergeometric functions can then be calculated by asymptotic expansions which are derived below. These expansions converge even faster than the series expansion; for all calculations in the present paper a number of $M = 2$ and $N = 3$ terms (see eq A.6) were sufficient. The use of the series and asymptotic expansion for the calculation of form factors will be illustrated below (Figure 7).

A.1. Asymptotic Expansion of the Excluded Volume Chain. The sum in eq 4.12 can be written in the form

$$\sum_{n=0}^{\infty} \frac{\Gamma(a+bn)(-x)^n}{\Gamma(d/2+n)(1+2\nu n)(2+2\nu n)n!} \quad (A.1)$$

Table 3. Some Useful Relations for Functions $f(x)$ Averaged over the Schulz Distribution ($u = x/(z + 1)$)

$f(x)$	$\langle f(x)\rangle_{SZ}$
x^n	$\frac{\Gamma(z+n+1)}{\Gamma(z+1)}u^n$
$\cos(ax)x^n$	$\frac{\Gamma(z+n+1)}{\Gamma(z+1)}u^n\frac{\cos[(z+n+1)\arctan(au)]}{(1+a^2u^2)^{(z+n+1)/2}}$
$\sin(ax)x^n$	$\frac{\Gamma(z+n+2)}{\Gamma(z+1)(z+n+1)}u^n\frac{\sin[(z+n+1)\arctan(au)]}{(1+a^2u^2)^{(z+n+1)/2}}$
$\cos^2(ax)x^n$	$\frac{\Gamma(z+n+1)}{\Gamma(z+1)}\frac{u^n}{2}\left(1+\frac{\cos[(z+n+1)\arctan(2au)]}{(1+4a^2u^2)^{(z+n+1)/2}}\right)$
$\sin^2(ax)x^n$	$\frac{\Gamma(z+n+3)}{\Gamma(z+1)(z+n+1)(z+n+2)}\frac{u^n}{2}\left(1-\frac{\cos[(z+n+1)\arctan(2au)]}{(1+4a^2u^2)^{(z+n+1)/2}}\right)$
$\cos(ax)\sin(ax)x^n$	$\frac{\Gamma(z+n+2)}{\Gamma(z+1)(z+n+1)}\frac{u^n}{2}\frac{\sin[(z+n+1)\arctan(2au)]}{(1+4a^2u^2)^{(z+n+1)/2}}$

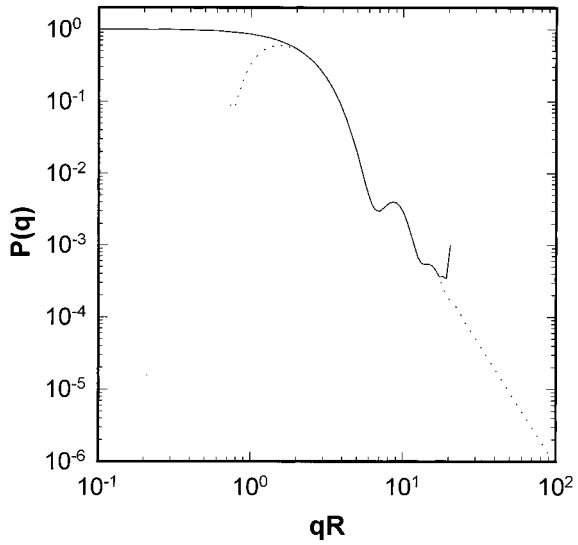

Figure 7. Hypergeometric function for $d = 3$ and $\alpha = -4/3$ (eq 3.10) calculated via the series expansion (solid line) and the asymptotic expansion (dotted line). By changing from the series to the asymptotic expansion, one calculates the function over the entire q-range.

This sum can be represented as a Barnes type contour integral

$$= \int_{c-i\infty}^{c+i\infty}\frac{ds}{2\pi i}\frac{\Gamma(a-bs)\Gamma(s)x^{-s}}{\Gamma(d/2-s)(1-2\nu s)(2-2\nu s)} \quad \text{(A.2)}$$

over the corresponding integrand $f(s)$. The integrand has simple poles at $s = -n$, $s = (2\nu)^{-1}$, $s = \nu^{-1}$, and $s = (a + n)/b$ where $n = 0, 1, ..., \infty$ is integer. The contour of integration separates the poles at $s = -n$ from all other poles. Evaluating the integral by summing over the residues of the poles at $s = -n$ immediately leads to (A.1).

In order to calculate the asymptotic expansion we simply flip over the path of integration and evaluate the residues of the function f at the remaining poles s_m, safely neglecting exponentially small terms. This leads to

$$= \sum_m \mathrm{Res}[f(s_m)]$$

$$= \frac{\Gamma[a-b/(2\nu)]\Gamma[1/(2\nu)]}{2\nu\Gamma[d/2-1/(2\nu)]}x^{-1/(2\nu)} - \frac{\Gamma[a-b/\nu]\Gamma[1/\nu]}{2\nu\Gamma[d/2-1/\nu]}x^{-1/\nu} + \sum_{n=0}^{\infty}\frac{b\Gamma[(a+n)/b]}{2[b-2\nu(a+n)][b-\nu(a+n)]\Gamma[d/2-(a+n)/b]}\times\frac{(-1)^n}{n!}x^{-(a+n)/b} \quad \text{(A.3)}$$

In the same way one obtains the asymptote of the polydisperse excluded volume chain. The sum in eq 4.17 can be written as

$$\sum_{n=0}^{\infty}\frac{\Gamma(a+bn)\Gamma(z+1+2\nu n)(-x)^n}{\Gamma(d/2+n)(1+2\nu n)(2+2\nu n)n!} \quad \text{(A.4)}$$

The corresponding contour integral has simple poles at $s = -n$, $s = (2\nu)^{-1}$, $s = \nu^{-1}$, $s = (a + n)/b$, and $s = (z + 1 + n)/(2\nu)$ where $n = 0, 1, ..., \infty$. Summation of the residues leads to

$$= \frac{\Gamma[a - b/(2\nu)]\Gamma[1/(2\nu)]\Gamma[z]}{2\nu\Gamma[d/2 - 1/(2\nu)]} x^{-1/(2\nu)} - \frac{\Gamma[a - b/\nu]\Gamma[1/\nu]\Gamma[z-1]}{2\nu\Gamma[d/2 - 1/\nu]} x^{-1/\nu} + \sum_{n=0}^{\infty} \frac{b\Gamma[(a+n)/b]\Gamma[z+1-2\nu(a+n)/b]}{2[b - 2\nu(a+n)][b - \nu(a+n)]\Gamma[d/2 - (a+n)/b]} \times \frac{(-1)^n}{n!} x^{-a/b} + \sum_{n=0}^{\infty} \frac{\Gamma[(z+1+n)/(2\nu)]\Gamma[a - b(z+1+n)/(2\nu)]}{2\nu(z+n)\,(z+n-1)\Gamma[d/2 - (z+1+n)/(2\nu)]} \times \frac{(-1)^n}{n!} x^{-(z+1+n)/(2\nu)} \quad \text{(A.5)}$$

A.2. Asymptotic Expansion of the Hypergeometric Function $_1F_2$. The asymptotic expansion of the hypergeometric function $_1F_2$ consists of a nonoscillating part and an oscillating part. An approach similar to the one described in section A.1 leads to the nonoscillating part, here given in terms of a $_3F_0$ hypergeometric series. The calculation of the oscillating part proceeds by replacing the Γ-functions in the Barnes contour integral by their Stirling expansions as described in refs 49 and 50.

The procedure leads to the following result:

$$\frac{\Gamma(a)}{\Gamma(b_1)\Gamma(b_2)} {}_1F_2\left(a;b_1,b_2;-\frac{x^2}{4}\right) = \frac{\Gamma(a)}{\Gamma(b_1-a)\Gamma(b_2-a)} \times \left(\frac{x^2}{4}\right)^{-a} \left\{\sum_{m=0}^{M-1} d_m \left(-\frac{x^2}{4}\right)^m + O(x^{-2M})\right\} + \pi^{-1/2}\left(\frac{x}{2}\right)^c \times \left\{\sum_{n=0}^{N-1} e_n x^{-n} \cos\left[x + \frac{\pi}{2}(c+n)\right] + O(x^{-N})\right\} \quad \text{(A.6)}$$

where both series are to be truncated at meaningful M and N.

The coefficients c, d_m, and e_n are given by

$$c = a - b_1 - b_2 + 1/2$$

$$d_m = \frac{(a)_m(1 + a - b_1)_m(1 + a - b_2)_m}{m!}$$

$$e_0 = 1$$

$$e_1 = \frac{3}{8} - (b_1 + b_2) + \frac{(b_1 - b_2)^2 - 3a^2 + 2a(1 + b_1 + b_2)}{2} \quad \text{(A.7)}$$

It is straightforward to calculate the higher order e_n, however, leading to quite lengthy expressions. For eq 3.12 one needs to average products of hypergeometric functions over the Schulz-Zimm distribution. When using the asymptotic expansion (A.6), the following relations are useful

$$\langle\cos(d_i + p_i x)\cos(d_j + p_j x)x^{e_i+e_j}\rangle = \frac{1}{2}[\cos(d_i + d_j) \times \langle\cos[(p_i + p_j)x]x^{e_i+e_j}\rangle + \cos(d_i - d_j) \times \langle\cos[(p_i - p_j)x]x^{e_i+e_j}\rangle - \sin(d_i + d_j)\langle\sin[(p_i + p_j)x]x^{e_i+e_j}\rangle - \sin(d_i - d_j)\langle\sin[(p_i - p_j)x]x^{e_i+e_j}\rangle] \quad \text{(A.8)}$$

$$\langle\cos(d_i + p_i x)x^{e_i+e_j}\rangle = \cos(d_i)\langle\cos(p_i x)x^{e_i+e_j}\rangle - \sin(d_i)\langle\sin(p_i x)x^{e_i+e_j}\rangle \quad \text{(A.9)}$$

The averaged trigonometric functions $\langle\sin(ax)x^n\rangle$ and $\langle\cos(ax)x^n\rangle$ are summarized in Table 3 where $u = x/(z + 1)$.

For the calculation of the functions $F_\alpha(q,R)$ over the entire q-range, one uses the series expansion (3.12) for low q-values and the asymptote (A.6) for large q-values as illustrated in Figure 7.

References and Notes

(1) Halperin, A.; Tirrell, M.; Lodge, T. P. *Adv. Polym. Sci.* **1992**, *31*, 100.
(2) Alexander, S. *J. Phys. (Paris)* **1977**, *38*, 983.
(3) de Gennes, P.-G. *J. Phys. (Paris)* **1976**, *37*, 1443.
(4) Milner, S.; Witten, T.; Cates, M. *Europhys. Lett.* **1988**, *5*, 413.
(5) Zhulina, E. B.; Borisov, O. V.; Pryamitsin, V. A. *J. Colloid Interface Sci.* **1990**, *137*, 495.
(6) de Gennes, P.-G. *Scaling Concepts in Polymer Physics*; Cornell University Press: Ithaca, NY, 1979.
(7) Evens, J. M. In *Light Scattering from Polymer Solutions*; Huglin, M. B., Ed.; Academic Press: New York, 1972.
(8) Glatter, O. *Acta Phys. Austriaca* **1977**, *47*, 83.
(9) Glatter, O. *J. Appl. Crystallogr.* **1977**, *10*, 415.
(10) Glatter, O. *J. Appl. Crystallogr.* **1980**, *13*, 577.
(11) Glatter, O. *J. Appl. Crystallogr.* **1981**, *14*, 101.
(12) For a summary see: Burchard, W. *Adv. Polym. Sci.* **1983**, *48*, 1.
(13) Auvray, L.; Auroy, P. In *Neutron, X-Ray and Light Scattering*; Lindner, P., Zemb, Th., Eds.; Elsevier: Amsterdam, 1991; p 199.
(14) Auroy, P.; Mir, Y.; Auvray, L. *Phys. Rev. Lett.* **1992**, *69*, 93.
(15) Hayter, J. B. In *Physics of Amphiphiles: Micelles, Vesicles and Microemulsions*; Degiorgio, V., Corti, M., Eds.; North-Holland: Amsterdam, 1985; p 59.
(16) Huang, J. S.; Sung, J.; Wu, X.-L. *J. Colloid Interface Sci.* **1989**, *132*, 34.
(17) Mittelbach, P.; Porod, G. *Acta Phys. Austriaca* **1961**, *14*, 405.
(18) Pedersen, J. S.; Gerstenberg, M. C. *Macromolecules* **1996**, *29*, 1363.
(19) Lodge, T. P.; Xu, X.; Ryu, C. Y.; Hamley, I. W.; Fairclough, J. P. A.; Ryan, A. J.; Pedersen, J. S. *Macromolecules* **1996**, *29*, 5955.
(20) Feigin, L. A.; Svergun, D. I. *Structure Analysis by Small-Angle X-Ray and Neutron Scattering*; Plenum Press: New York, 1987.
(21) Luke, Y. L. *The Special Functions and Their Approximations*; Academic Press: New York, 1969.
(22) Seaborn, J. B. *Hypergeometric Functions and Their Applications*; Springer: New York, 1991.
(23) Pedersen, J. S.; Posselt, D.; Mortensen, K. *J. Appl. Crystallogr.* **1990**, *23*, 321.
(24) Aragon, S. R.; Pecora, R. *J. Chem. Phys.* **1976**, *64*, 2395.
(25) Schulz, G. V. *Z. Phys. Chem.* **1939**, *43*, 25.
(26) Daoud, M.; Cotton, J. P. *J. Phys. (Paris)* **1982**, *43*, 531.
(27) Shusharina, N. P.; Nyrkova, I. A.; Khokhlov, A. R. *Macromolecules* **1996**, *29*, 3167.
(28) Rayleigh, J. W. *Proc. R. Soc. London* **1914**, *A90*, 219.
(29) Neugebauer, T. *Ann. Phys.* **1943**, *42*, 509.
(30) Kratky, O.; Porod, G. *J. Colloid Sci.* **1949**, *4*, 35.
(31) Förster, S.; Wenz, E.; Lindner, P. *Phys. Rev. Lett.* **1996**, *77*, 95.

(32) Richter, D.; Jucknischke, O.; Willner, L.; Fetters, L. J.; Lin, M.; Huang, J. S.; Roovers, J.; Toporovski, C.; Zhou, L. L. *J. Phys. IV* **1993**, *3*, 3.
(33) Dozier, W. D.; Huang, J. S.; Fetters, L. J. *Macromolecules* **1991**, *24*, 2810.
(34) des Cloizeaux, J. *Phys. Rev. A* **1974**, *10*, 1665.
(35) des Cloizeaux, J. *J. Phys. (Paris)* **1985**, *41*, 223.
(36) Bishop, M.; Clarke, J. H. R. *J. Chem. Phys.* **1991**, *94*, 3936.
(37) Valleau, J. P. *J. Chem. Phys.* **1996**, *104*, 3071.
(38) Fisher, M. *J. Phys. Soc. Jpn.* **1969**, *26*, (Suppl.) 44.
(39) Macdonald, D.; Hunter, D. L.; Kelly, K.; Jan, N. *J. Phys. A* **1992**, *25*, 1429.
(40) Ptitsyn, O. B. *Zh. Fiz. Khim.* **1957**, *31*, 1091.
(41) Benoit, H. C. *R. Acad. Sci.* **1957**, *245*, 2244.
(42) McIntyre, D.; Mazur, J.; Wims, A. M. *J. Chem. Phys.* **1968**, *49*, 2896.
(43) Utiyama, H.; Tshunashima, Y.; Kurate, M. *J. Chem. Phys.* **1971**, *55*, 3133.
(44) des Cloiseaux, J.; Jannink, G. *Polymers in Solution*; Clarendon Press: Oxford, 1990.
(45) Pedersen, J. S.; Schurtenberger, P. *Macromolecules* **1996**, *29*, 7602.
(46) Wittkop, M.; Kreitmeier, S.; Göritz, D. *J. Chem. Phys.* **1996**, *104*, 351.
(47) Debye, P. *J. Phys. Colloid Chem.* **1947**, *51*, 18.
(48) Leube, W. Ph.D. Thesis, University of Potsdam, 1997.
(49) Wright, E. M. *J. London Math. Soc.* **1935**, *10*, 286.
(50) Braaksma, B. L. *J. Comp. Math.* **1963**, *15*, 239.

MA970761V